MEASUREMENTS OF THE DIRECTIONS OF PROPAGATION VECTOR AND POYNTING FLUX OF AURORAL HISS BY MEANS OF THE S-310JA-5 ROCKET

Iwane KIMURA, Toshio MATSUO,

Department of Electrical Engineering II, Kyoto University, Yoshida-honmachi, Sakyo-ku, Kyoto 606

Koichiro TSURUDA

Institute of Space and Aeronautical Science, University of Tokyo, Komaba 4-chome, Meguro-ku, Tokyo 153

and

Hisao YAMAGISHI

National Institute of Polar Research, 9-10, Kaga 1-chome, Itabashi-ku, Tokyo 173

Abstract: Directions of the propagation vector and the Poynting flux of auroral hiss at 7 kHz were measured by the S-310JA-5 rocket launched on 10 June 1978 from Syowa Station in Antarctica.

The observation of the ratio of magnetic field intensity to electric field intensity of the hiss as well as the above-mentioned measurements result in a conclusion that the hiss has propagated down to the rocket with a large wave normal angle to the geomagnetic field so that the source region must be located in the vicinity of the altitudes of the rocket apex.

The time variation of the hiss intensity showed a relatively good correlation with the flux of 4.45 keV electrons with pitch angles from 3° to 34°.

1. Introduction

The relationship between an aurora and VLF emissions has been investigated for a long time by ground observations (*e.g.* MOROZUMI, 1965; OGUTI, 1975), by satellites (MOSIER and GURNETT, 1971; MOSIER, 1971) and by rockets (*e.g.* UNGSTRUP, 1971). The high correlation has already been found between these two especially for a burst type of hiss and some type of chorus. These results suggest that some type of VLF emission, that is auroral hiss, may be generated at altitudes of the lower ionosphere where the auroral brightness becomes maximum. However, the source region of such VLF emissions has not yet been clarified.

At Syowa Station (69.0°S, 39.6°E in geographic and 70.4°S, 79.4°E in geomagnetic coordinates) in Antarctica, many rockets were launched in order to investigate the wave and the particle relationship (*e.g.* KIMURA *et al.*, 1980). S-310JA-5 is one

of the rockets having such an objective. It was launched into the coronal aurora at 2256:50 UT on 10 June 1978.

The Poynting flux and the propagation vector direction of auroral hiss at a frequency of 7 kHz were measured with energetic electrons having energies less than 10 keV. This report describes briefly the instruments on board and the results of the experiments.

2. Instruments on Board the Rocket

The instruments on board the S-310JA-5 rocket to measure VLF emissions are called PWL-PFX. The PWL stands for a low frequency plasma wave measurement and the PFX stands for Poynting flux measurement. The block diagram of PWL-PFX is shown in Fig. 1. Namely, two pairs of dipole antennas (each 2.4 m tip-to-tip) and a set of crossed loop antennas (each 10 cm$\phi \times 100$ turns; an effective length of 0.6 mm including transformer turn ratio) are used for picking up the electric (E) and the magnetic (B) field components of the waves. The instruments assembled in the nose cone and the extended antennas are shown in Fig. 2.

2.1. *Wide band spectra*

First of all, VLF wide band spectra were taken from the preamplifier of the E_x channel and from that of B_y channel and were fed by a time sharing (10 s for E and 5 s for B) to a common wide band amplifiier with AGC and sent to the ground by a

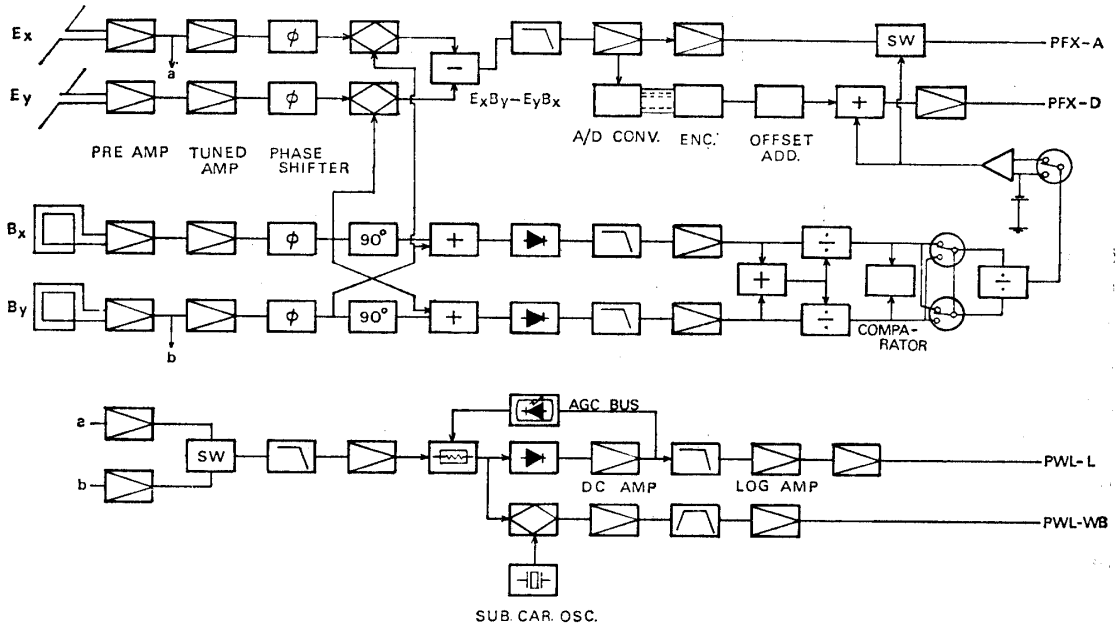

Fig. 1. Block diagram of PWL-PFX.

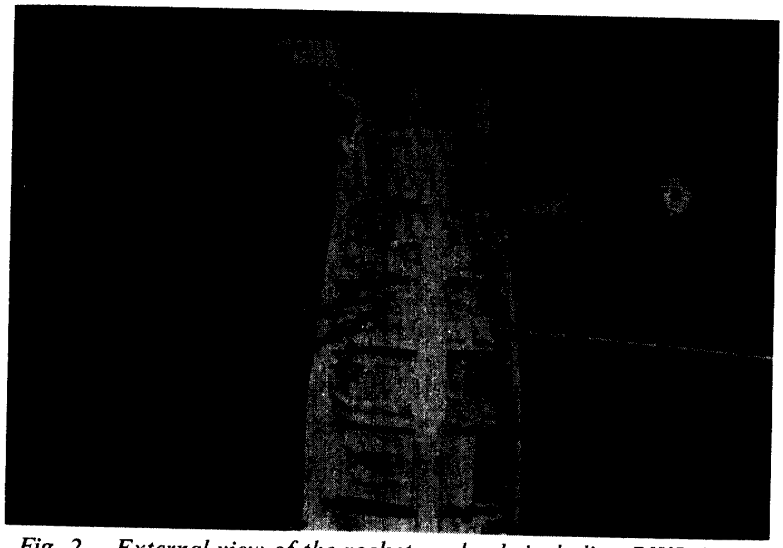

Fig. 2. External view of the rocket payloads including PWL-PFX.

wide band (WB) telemeter. The AGC level (PWL-L) was amplified with a Log Amp and was sent to the ground as the envelope level of wide band spectra.

2.2. *Measurement of propagation ($\vec{k}$) vector*

For the $\vec{k}$-vector measurement, the x and y components of the magnetic field of waves, B_x and B_y, picked up by the crossed loop antennas are amplified by the tuned amplifier at 7 kHz with a band width of 100 Hz, where the Z direction is the direction of the rocket axis (see Fig. 3). To these two components, those of 90° phase shifted from the former are added and the composed envelopes, that is $B_x + B_y(\pi/2)$ and $B_y + B_x(\pi/2)$, are obtained. By the use of an adder, a divider and a comparator, the quantity

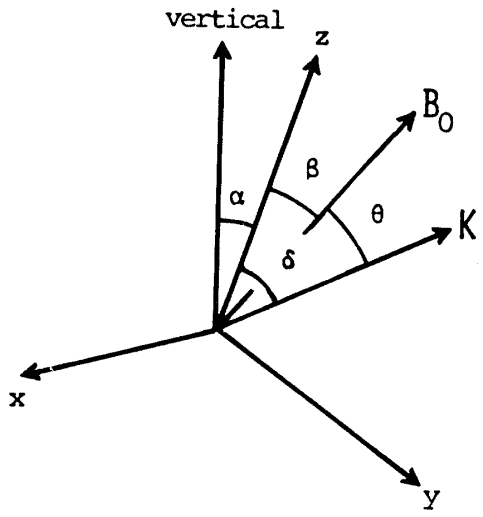

Fig. 3. $\vec{k}$-vector, rocket axis and geomagnetic field directions in the coordinate system, in which the rocket axis is directed along the Z axis.

$$\varepsilon \equiv \frac{B_x(\pi/2)+B_y}{B_x+B_y(\pi/2)} \tag{1}$$

is calculated.

For a $\vec{k}$-vector making an angle δ from the rocket axis the above quantity must be equal to

$$\varepsilon = \frac{1-\cos\delta}{1+\cos\delta} \tag{2}$$

because the magnetic field components of the whistler mode wave are circularly polarized in the plane perpendicular to the $\vec{k}$-vector direction in the ionosphere. We can, therefore, determine the angle δ from the calculated quantity ε.

2.3. *Measurements of Poynting flux*

For Poynting flux measurements, as shown in the top channel of Fig. 1, the quantity $E_xB_y - E_yB_x$ is calculated from B_x and B_y mentioned above and E_x and E_y which are picked up by a set of crossed dipole antennas and are amplified by the tuned amplifier at 7 kHz. Then 7 kHz and higher frequency components are removed from the above quantity by a LPF whose cut off frequency is 100 Hz.

Namely, this filtered output must be a time average within 10 ms of the rocket axial (z) component of the Poynting flux. It is digitized by an A/D converter and then sent to the ground through an analog telemeter channel.

3. S-310JA-5 Rocket Experiment

The S-310JA-5 rocket was launched at 2256 UT on 10 June (or at 0156 LT on 11 June), 1978 in the direction of the local geomagnetic field lines. It was plunged into a coronal aurora, and reached an altitude of 226 km at 235.7 s after launch. The time was in a small scale geomagnetic substorm, the magnitude of which was -150 nT.

The rocket hit a bright aurora during its flight, as shown in Figs. 4 and 5 (after HIRASAWA). Fig. 4 shows the aurora taken by the ground-based all sky camera, where the rocket position is indicated by a black dot. Fig. 5 shows the rocket trajectory together with the 5577 Å equicontour curves. Ground observations of VLF wave phenomena indicated that from 5 or 6 min before the launching the frequency components around 8 kHz suddenly increased but decreased again just after launch, as shown in Fig. 6. This emission must be a kind of auroral hiss. Cosmic noise absorption (CNA) measurements, also shown in Fig. 6, indicated a slight increase of the absorption less than 1 dB.

The VLF wide band spectrum observed by the rocket is shown in Fig. 7, which indicates a time sharing display of the electric and the magnetic field components of

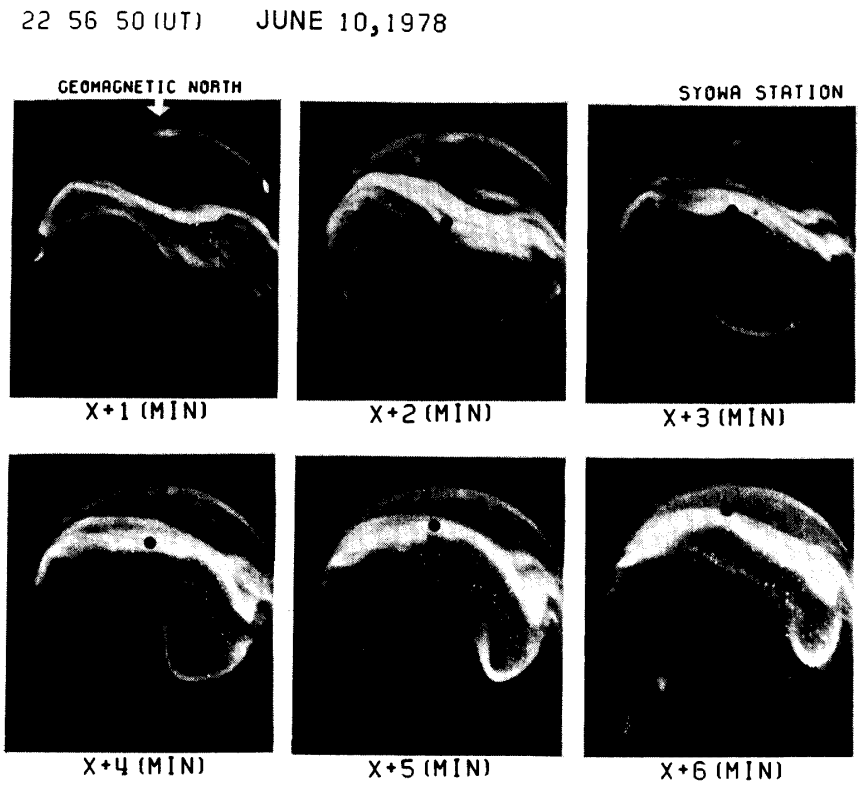

Fig. 4. Auroral pictures by an all sky camera at 6 different times during flight. Rocket location is shown by black dots.

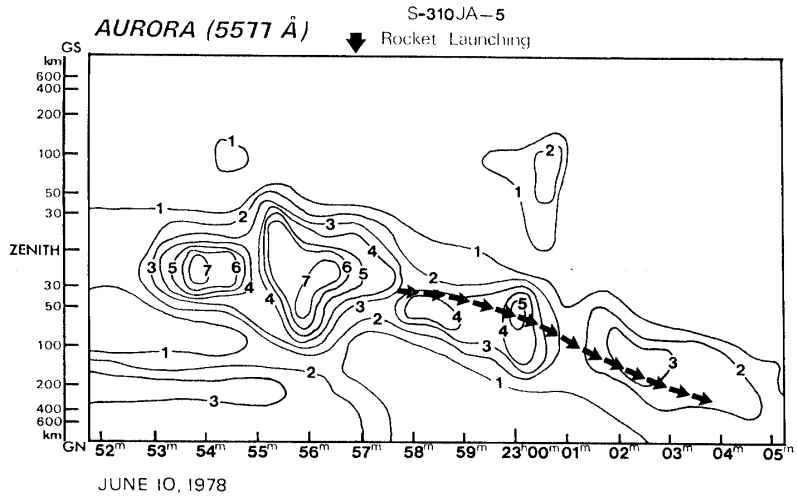

Fig. 5. Equicontour curves of 5577 Å strength with time. The rocket trajectory is shown by solid arrows. The parameters associated with each line denote the 5577 Å intensity in kR (after HIRASAWA).

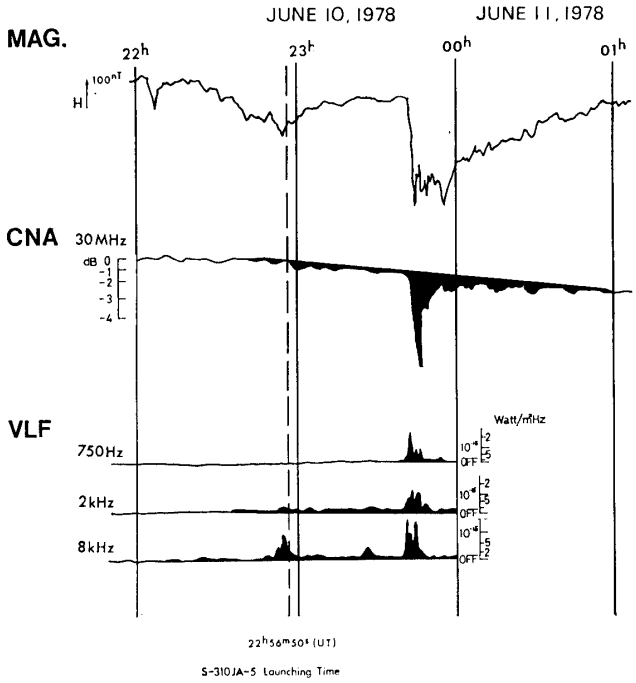

Fig. 6. Time variations of geomagnetic field, CNA and VLF noise intensities at 0.75, 2 and 8 kHz, all observed on the ground.

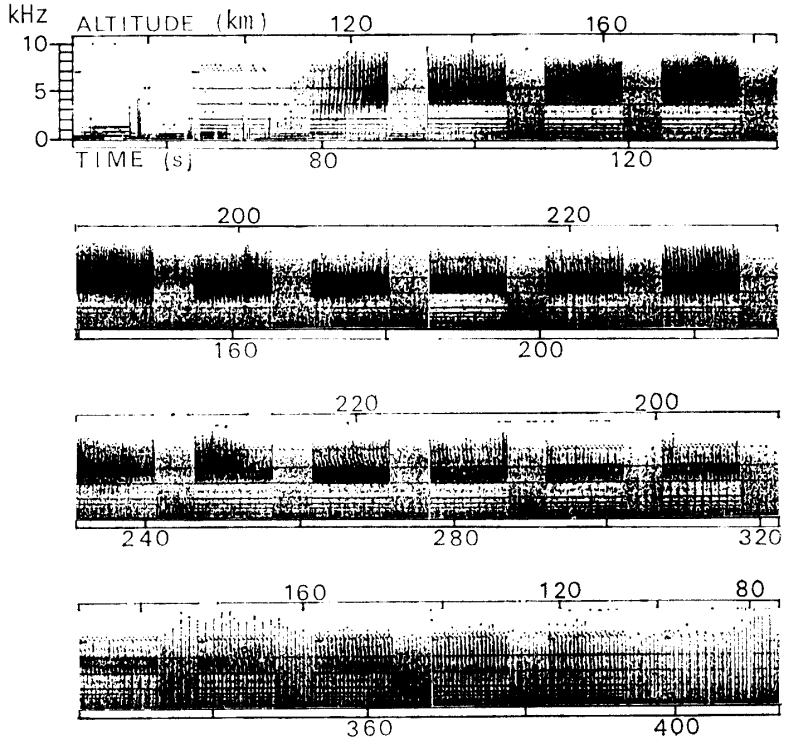

Fig. 7. Wide band VLF spectra observed by the S-310JA-5 rocket.

the wide band spectrum; 10 s for E and 5 s for B component. From this figure, an intense hiss with frequencies from 3.5 to 8 kHz is seen in both E and B components for altitudes above 120 km.

The emissions have a sharp lower cutoff around 3.5 kHz. The band width becomes smaller and the signal intensity becomes weaker with time after $t=160$ s, although a fluctuation in spectrum arises at around $t=240$ s.

3.1. *Hiss intensity*

The wide band VLF data were digitized by an A/D converter with a sampling period of 50 μs and their frequency spectrum was obtained by a computer with FFT program. A hiss intensity at a certain frequency was then determined from the Fourier transform of the wide band signal.

For example, Figs. 8 and 9 show the altitude variations of the quantities E and cB at 7 kHz and 5 kHz respectively, where E is the electric field (in dB on μV/m) and cB is the light velocity c times the magnetic flux density B, which has the same dimension with E. The B component for an altitude below 180 km of the descending leg is suffering from some interference, so that the quantity shown is not reliable.

If the propagation is in the whistler mode along the geomagnetic field line, the

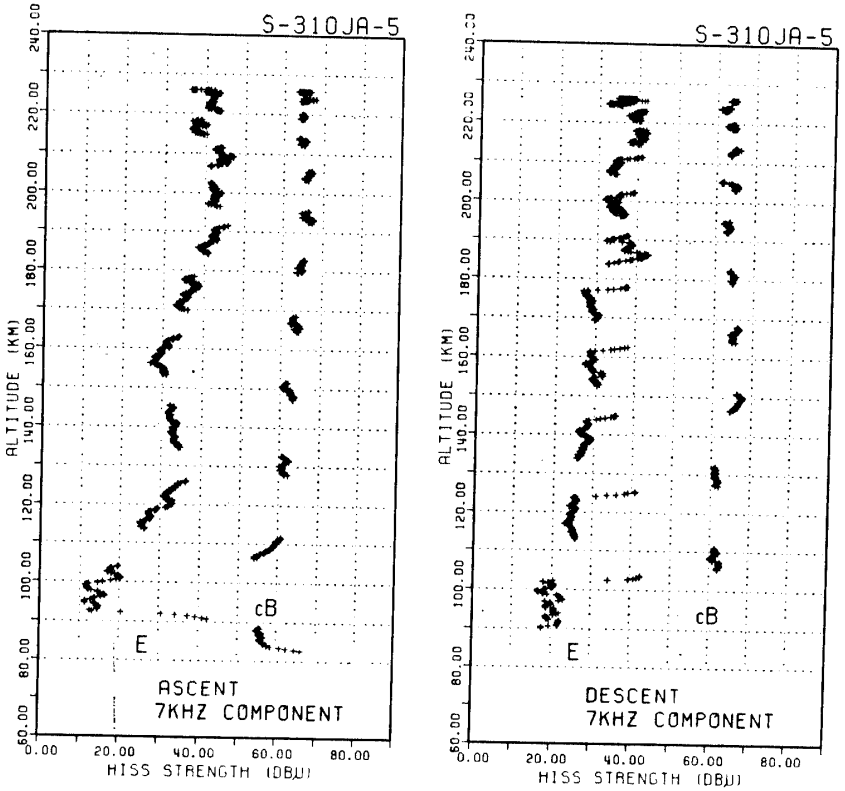

Fig. 8. Altitude variations of the quantities E and cB at 7 kHz.

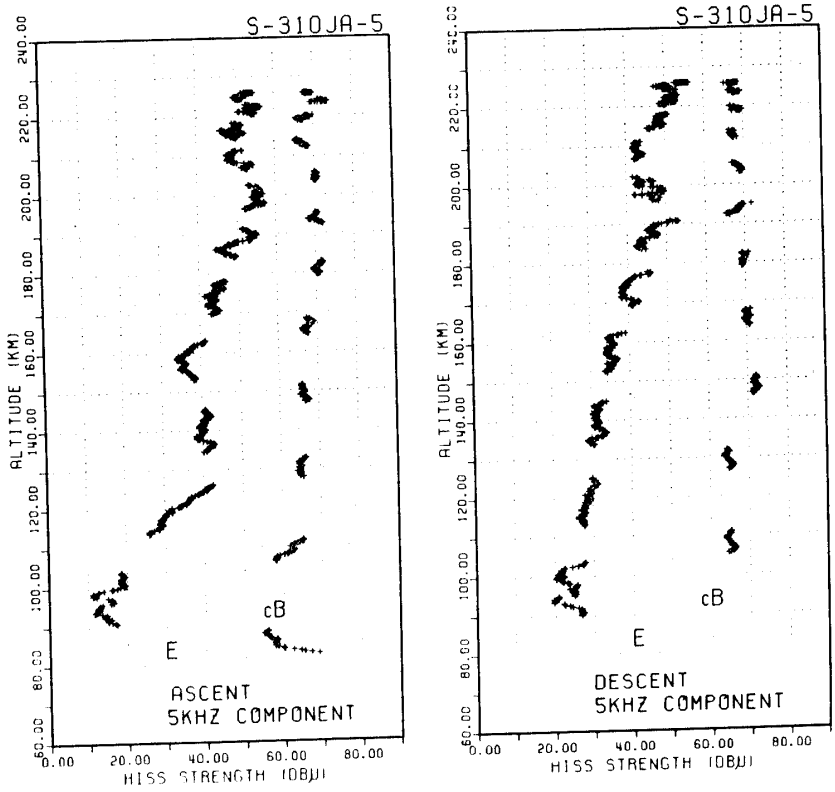

Fig. 9. Altitude variations of the quantities E and cB at 5 kHz.

ratio of cB to E must be the refractive index for the propagating mode.

Due to the time sharing, there is either E or cB, so that the exact ratio cB/E can not be taken at each altitude. But from the trend of altitude variations shown in Figs. 8 and 9, the ratio for the 7 kHz emissions, for example, is 30 at $h=150$ km and 12.6 at 200 km for ascent which are much smaller than the calculated refractive index using the observed electron density for purely longitudinal propagations; *e.g.* 50 at 150 km and 42 at 200 km. The situation is almost the same for 5 kHz. This discrepancy is understandable if the angle θ between the $\vec{k}$-vector and the geomagnetic field is large near the resonance cone angle. Therefore, the propagation mode of the observed emissions must be the whistler mode for both 7 and 5 kHz, provided that the propagation angle θ is large.

As shown in Fig. 7, the E field components are strongly suffering from spin modulation, peaking twice per spin period, whereas the B field components are not so much affected by the rocket spin motion. This characteristic is not contradictory to the result of E field, if the propagation angle θ is large, because in such a case the E field is almost linearly polarized while the B field is almost circularly polarized.

It is interesting to note that the spin modulation of the E component has shown a dispersion-like characteristic for altitudes around 223 km for the descending leg

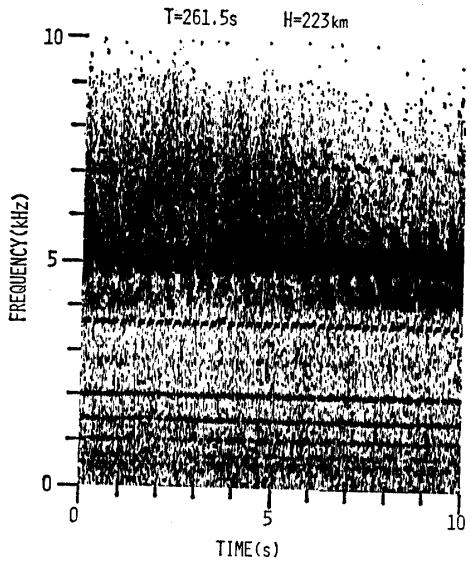

Fig. 10. Spin-modulated E field spectrum showing a dispersion-like characteristic.

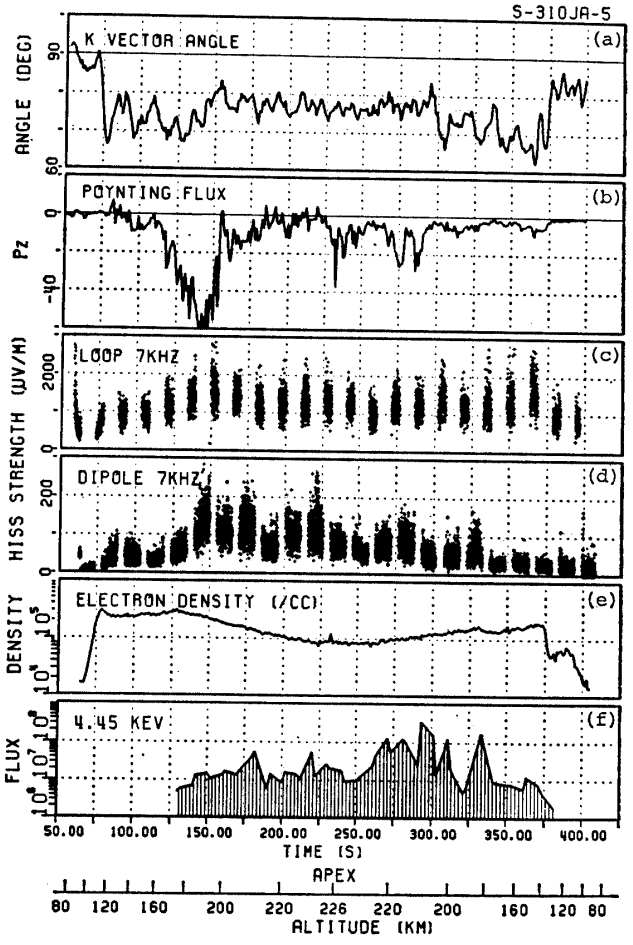

Fig. 11. Time variations of the quantities observed by the rocket.
(a) $\vec{k}$-vector angle of the 7 kHz component from the rocket axis direction.
(b) Rocket-axial component of Poynting flux.
(c) and (d) The wave magnetic flux density B multiplied by the light speed c, and the wave electric field intensity E, both in the same unit $\mu V/m$.
(e) Electron density measured by an impedance probe (after OYA and TAKAHASHI).
(f) 4.45 keV component of energetic electrons with a pitch angle of 3°~34° measured by an electrostatic electron channel multiplier type analyzer (after KAYA and MATSUMOTO).

as illustrated in Fig. 10. This characteristic may be caused by a frequency dependence of the arrival azimuth direction.

In Fig. 11, the cB and E components are again shown in (c) and (d) for comparison with other observed quantities which will be explained later. In (c) and (d), each point represents an average of the Fourier components in the frequency range of 7 ± 0.14 kHz at every 25.6 ms.

3.2. $\vec{k}$-vector direction

The $\vec{k}$-vector angle of the 7 kHz hiss component, which is represented by the angle between the $\vec{k}$-vector direction and the rocket spin axis, is shown in Fig. 11(a). Below an altitude of 100 km, the magnetic field intensity was so weak that the $\vec{k}$-vector angle around 90° is erroneous. It turns out that the altitude range in which the $\vec{k}$-vector direction was reasonably measured is just the same range where the electron density was higher than 10^5 cm^{-3}, so that the wave magnetic field intensity was magnified. Above this level, the $\vec{k}$-vector fluctuated in the range from 65° to 85°, whose average value changes slowly with altitude. On the other hand, the time variation of the angle α (see Fig. 3) between the rocket axis and the vertical direction is shown in Fig. 12(a) (after TOYODA and ISHIDO). Taking account of this figure, we can estimate a possible range of the angle between the $\vec{k}$-vector and the vertical direction. Fig. 12(b) indicates the maximum and minimum of that angle. It appears that the direction of $\vec{k}$ was making a large angle with the vertical direction.

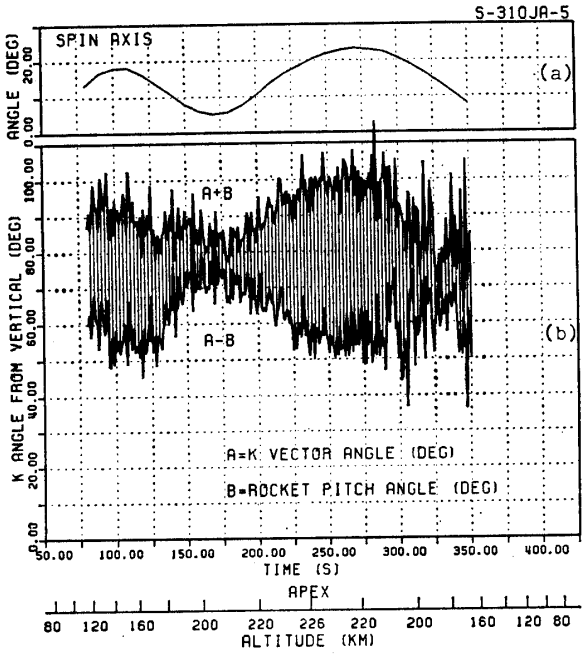

Fig. 12. (a) The time variation of the rocket pitch angle that is the angle of the rocket axis from the vertical. (b) Estimated $\vec{k}$-vector angle measured from the vertical. The hatched area shows an ambiguity between the possible, maximum and minimum values of the above $\vec{k}$-vector angle.

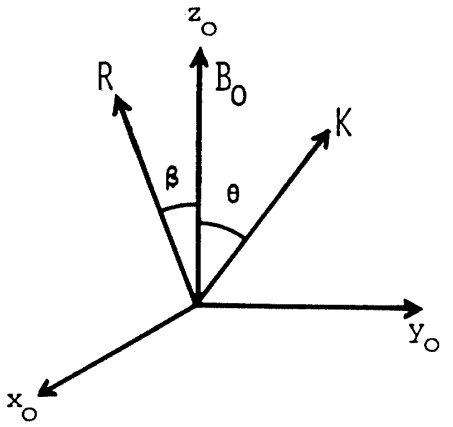

Fig. 13. A different rectangular coordinate system, where Z_0 axis is directed along the geomagnetic field.

3.3. Poynting flux

As was explained in Section 2, one component of the Poynting flux, *i.e.* the rocket axial component $P_z = E_x B_y - E_y B_x$ was calculated on board, where the z axis was directed in the rocket axial direction in a rectangular coordinate system as shown in Fig. 3. This P_z had components with frequencies less than 100 Hz by the LPF.

On the other hand, let us choose a different rectangular coordinate system as shown in Fig. 13, where the Z_0 axis is directed along the geomagnetic field B_0. The angle between the Z_0 axis and the rocket axis is denoted by β. The components of the Poynting vector in x_0, y_0, z_0 axes are denoted by P_{x0}, P_{y0}, P_{z0}. Then the P_z component observed by the rocket can be represented by P_{x0}, P_{y0} and P_{z0} as follows;

$$P_z = -\sin\beta \sin\Omega t\, P_{x0} + \sin\beta \cos\Omega t\, P_{y0} + \cos\beta\, P_{z0} \tag{3}$$

where Ω is the angular frequency of the rocket spin. Therefore, if the original Poynting flux is assumed constant with time, the above P_z should be composed of a DC component $\bar{P}_z$, *i.e.*

$$\bar{P}_z = \cos\beta\, P_{z0} \tag{4}$$

and an AC or a spin frequency component with amplitude

$$\tilde{P}_z = \sin\beta \sqrt{P^2_{x0} + P^2_{y0}} \tag{5}$$

so that $\bar{P}_z$ and $\tilde{P}_z$ must be separately estimated by the Fourier analysis of the P_z signal.

If $\bar{P}_z$ and $\tilde{P}_z$ can be determined, then P_{z0} and $\sqrt{P^2_{x0} + P^2_{y0}}$ or the angle α between B_0 and the Poynting vector is calculated by

$$\alpha = \tan^{-1} \sqrt{P^2_{x0} + P^2_{y0}} / P_{z0} \tag{6}$$

because the angle β is known by another measurement.

According to MOSIER and GURNETT (1971), the P_{z0} component is represented by

$$P_{z0}=\frac{1}{2}\frac{E^2_0}{\mu_0 c}\, n\cos\theta\left[\frac{P}{P-n^2\sin\theta}+\left(\frac{D}{S-n^2}\right)^2\right] \tag{7}$$

where E_0 is the electric field intensity, μ_0 the permeability, c the light velocity, n the refractive index, and θ the angle between B_0 and the $\vec{k}$ vector. P, S, and D are the known quantities defined by STIX (1962). That is

$$P=1-f^2_p/f^2,\ S=2-2f^2_p/(f^2-f^2_H),\ D=2f^2_p f_H/f(f^2-f^2_H) \tag{8}$$

where f is the wave frequency, f_p and f_H are the electron plasma and the cyclotron frequency respectively.

The quantities in brackets of eq. (7) are always positive for the whistler mode, so that the polarity of P_{z0} is identical to the polarity of cos θ. Namely, if P_{z0} is negative, θ must be larger than 90°, that is, the Poynting energy is directed downwards.

In our rocket measurement, the DC component of P_z, that is $\bar{P}_z$ was obtained by selecting the zero frequency component out of an FFT spectrum of P_z. Fig. 11(b) illustrates the $\bar{P}_z$ component. Actually, when the original Poynting flux is a time varying quantity, then the above $\bar{P}_z$ must be the time average of cos β P_{z0}.

As shown in Fig. 11(b), the polarity of $\bar{P}_z$ is always negative, so that θ must be larger than 90°, or the Poynting vector is directed downwards. The magnitude of $\bar{P}_z$ becomes maximum when both E and B become maximum as shown in Fig. 11(c) and (d). The absolute magnitude of P_z in the unit of W/m² Hz is 1.14×10^{-13} times the ordinate of the curve in (b), so that the maximum of $\bar{P}_z$ at $t=140$ s is 6.84×10^{-12} W/m² Hz.

Theoretically, from the magnitude of the spin frequency component of P_z and the DC component $\bar{P}_z$, the angle α between the Poynting vector and the geomagnetic field is to be determined, unless the Poynting flux is a time varying quantity. However, P_z was fluctuating with time, so that from the ratio of $\tilde{P}_z$ to $\bar{P}_z$ actually observed, no reasonable value of the angle α was deduced.

3.4. *Relationship with energetic electron flux*

On the S-310JA-5 rocket, an electrostatic analyzer with a channel electron multiplier was installed for the measurement of electrons with energies from 1 to 10 keV (KAYA *et al.*, 1981).

In Fig. 11(f), the particle flux at 4.45 keV with a pitch angle ranging from 3° to 34° is shown with time. Comparing this figure with the observed hiss strength (see Fig. 11(c) and (d)), the variation of electron flux from 175 to 290 s appears to have a relatively good correlation with the curve (d), that is, the E component of the emissions. For electrons with other energy and pitch angle in the observed energy range from 1 to 10 keV, the correlation is not so clear.

The above fact may suggest that the 4.45 keV electrons are responsible for the generation of a part of the observed emissions.

4. Discussion and Conclusion

The S-310JA-5 rocket was launched into a coronal aurora and hit an intense auroral arc during its flight. VLF band-limited hiss emissions with the frequencies from 3.5 to 7 kHz were observed. The following is the summary of the observed facts.

1) Time and/or altitude variations of the electric (E) and the magnetic (B) fields are simultaneous and consistent with each other, indicating that the E and the B components are of an electromagnetic mode.

2) From the ratio of the quantity cB to E, the propagation is considered as the whistler mode propagation, if it is in a direction making a large wave normal angle to the geomagnetic field direction.

3) The measurement of the $\vec{k}$-vector becomes possible for altitudes where the electron density is as high as 10^5 cm^{-3}. The $\vec{k}$ direction observed was making a large angle with the vertical direction.

4) The Poynting flux of the emissions comes downwards. The maximum flux is $\sim 7 \times 10^{-12}$ W/m^2 Hz.

5) Out of the energetic electrons measured in the range from 1 to 10 keV, 4.45 keV electrons with small pitch angles have a better correlation with the hiss intensity than the electrons with other energies and pitch angles do.

From these facts, it can be concluded that the band-limited emissions observed on the S-310JA-5 rocket were a type of auroral hiss propagating downwards with large wave normal angles to the geomagnetic field, and that the emissions were associated with precipitating electrons having energies around 4.45 keV, although the correlation was not very high.

The location of the emission source must be above the rocket apex according to the fact 4). However, from the fact 2) and 3), the wave normal must be in a direction making a large angle to the vertical direction, say $78° \pm 10°$ at an altitude of 205 km, as well as a large angle to the geomagnetic field, around the resonance cone angle ($\sim 90°$). This result is similar to that obtained by UNGSTRUP (1971).

Such a situation is not realized when the emission source is located far away from the rocket altitude, *e.g.* in the equatorial region in the magnetosphere.

It is rather possible that the source region is located around the altitude of the rocket apex. It is so concluded because $\bar{P}_z$ shown in Fig. 11(b) indicates large negative values only below the altitude of 200 km for ascent, in spite of the fact that B and E fields are not comparatively small for altitudes above 200 km.

The fact that the wave normal angle of the emissions is large will suggest that the emissions are generated by the Cerenkov type of radiation, perhaps by coherent Cerenkov radiations, by an electron beam (KIMURA, 1971; KUMAGAI *et al.*, 1980).

Acknowledgments

We wish to express our thanks to the members of the 19th wintering party of Japanese Antarctic Research Expedition, headed by Prof. T. HIRASAWA, for their effort in launching the rocket successfully into an auroral arc and for their data acquisition of ground-based geophysical observations.

We are grateful also to the following staff for providing us with the data observed by the same rocket; Prof. M. TOYODA and Dr. M. ISHIDO of Kobe University for the rocket aspect data, to Prof. H. MATSUMOTO and Mr. N. KAYA of Kobe University for the energetic electron flux data, to Prof. H. OYA and Mr. T. TAKAHASHI of Tohoku University for the electron density data by an impedance probe. We also acknowledge the courtesy of Prof. T. HIRASAWA who produced Fig. 5 and allowed us to use it in the present paper.

Finally the helpful comments given by Drs. H. MATSUMOTO and K. HASHIMOTO of Kyoto University on this paper are appreciated.

References

KAYA, N., MATSUMOTO, H. and YAMAGISHI, H. (1981): Rocket measurement of auroral keV electron fluxes in Antarctica. Mem. Natl Inst. Polar Res., Spec. Issue, **18**, 427–438.

KIMURA, I. (1971): Cerenkov instability and VLF emissions generated outside the plasmapause. Rep. Ionos. Space Res. Jpn, **25**, 360–368.

KIMURA, I., MATSUO, T., KAMADA, T. and NAGANO, I. (1980): Auroral hiss observed by Antarctic rockets, S-310JA-20 and 21. Nankyoku Shiryô (Antarct. Rec.), **69**, 17–36.

KUMAGAI, H., HASHIMOTO, K., KIMURA, I. and MATSUMOTO, H. (1980): Computer simulation of a Cerenkov interaction between obliquely propagating whistler mode waves and an electron beam. Phys. Fluids, **23**(1), 184–193.

MOROZUMI, H. M. (1965): Diurnal variation of auroral zone geophysical disturbances. Rep. Ionos. Space Res. Jpn, **19**, 286–298.

MOSIER, S. R. (1971): Poynting flux studies of hiss with Injun 5 satellite. J. Geophys. Res., **76**, 1713–1728.

MOSIER, S. R. and GURNETT, D. A. (1971): Theory of the Injun 5 very-low-frequency Poynting flux measurements. J. Geophys. Res., **76**, 972–977.

OGUTI, T. (1975): Metamorphoses of aurora. Mem. Natl Inst. Polar Res., Ser. A (Aeronomy), **12**, 101 p.

STIX, T. H. (1962): The Theory of Plasma Waves. New York, McGraw-Hill, 10.

UNGSTRUP, E. (1971): Rocket observation of VLF hiss in Aurora. Planet. Space Sci., **19**, 1475–1495.

(Received August 6, 1980)